ELSEVIER

Polymer 40 (1999) 4483–4492

polymer

Structure development during flow of ternary blends of a polyamide (nylon 66), a thermotropic liquid crystalline polymer (poly(ester amide)) and a functionalized polypropylene

Yongsok Seo*, Byeongyeol Kim, Kwang Ung Kim

Polymer Processing Laboratory, Korea Institute of Science and Technology (KIST), PO Box 131, Cheongryang, Seoul, South Korea 130-650

Received 15 April 1998; received in revised form 7 July 1998; accepted 8 September 1998

Abstract

It is shown that a fibril structure of a thermotropic liquid crystalline polymer (TLCP)(poly(ester amide)) can be developed in the shear flow field of a thermoplastic matrix (polyamide, nylon 66) when the viscosity of the latter is lower than that of the former. The addition of a third component, a functionalized polypropylene (maleic-anhydride-grafted polypropylene, MA-PP) that interacts with both the matrix polymer (nylon 66) and the thermotropic liquid crystalline polymer facilitates the structural development of the TLCP by acting as a compatibilizer at the interface. Morphological observations have demonstrated the significance of compatibilization in immiscible polymer blends. The compatibilizer brings about good adhesion at the interface, reduces the droplet size, and enables a finely dispersed liquid crystalline polymer to be deformed by shear flow without strong elongation, even when the viscosity of the matrix is much lower than that of the liquid crystalline polymer. The mechanical properties of the ternary blends are increased when a proper amount of MA-PP is added. This is attributed to fine strand generation induced by the addition of MA-PP. Enhanced adhesion at the interface invokes better elongation in the ternary blends.

Keywords: In situ formed compatibilizer; Shear induced deformation; Structure development

1. Introduction

The use of thermotropic liquid crystal polymers (TLCPs) in blends with other thermoplastics has been attractive for many reasons [1–14]. Upon melting, TLCPs give rise to highly organized liquid phases (mesophases) that tend to spontaneously pack parallel to one another to form highly oriented domains. Under elongational processing conditions, these oriented domains can develop a fibril morphology with a high degree of orientation, leading to enhanced mechanical properties [1–4]. This property enables TLCPs to be used as reinforcing fillers that are not present as a solid phase during processing of the composite, but are formed when the material is cooled to a solid state. These blends have been called in situ composites because of their in situ shaping during processing [2]. For special engineering plastics that can retain high viscosities at high processing temperatures (at least higher than the crystal–nematic transition temperature), and hence have high melt strength, the elongation process is readily applicable. In contrast, the melt viscosities for polymers produced by condensation reactions, such as polyamides (nylons) and polyesters, are usually two or three orders lower than those of TLCPs at processing temperatures and shear rates. All previous findings agree that some form of elongational deformation, as well as a matrix polymer with a higher viscosity than the TLCP phase, is necessary for the deformation of the TLCP phase [7–9]. Therefore, it is easy to predict that fine dispersion and fibril formation of TLCP will be very difficult in polyamides, one of the most widely used engineering plastics, because of both their immiscibility with TLCPs and their low viscosities at processing temperatures and shear rates. The lack of miscibility between TLCPs and polyamides leads to poor dispersion and thereby degrades some mechanical properties of these blends [2,4,10–12].

In this study, we examine the properties of blends comprised of a TLCP (Vectra B950, a poly(ester amide)), a polyamide (nylon 66), and a maleic-anhydride-grafted polypropylene (PP). Our goal is to gain an understanding of the structure development of the TLCP phase in ternary blends of nylon 66, TLCP, and a maleic-anhydride-grafted PP based on the molecular characteristics when the matrix viscosity is lower than the TLCP's viscosity. Since nylon 66 shows an interesting crystallization behavior when a

* Corresponding author.

0032-3861/99/$ - see front matter
PII: S0032-3861(98)00684-3

nucleating agent exists [13], ternary blends are expected to show interesting phenomenon, different from other polyamide blends [14,15].

2. Experimental

2.1. Materials

The chosen TLCP was an all aromatic liquid crystalline poly(ester amide), Vectra B950 (VB) (a copolymer based on 6-hydroxy-2 naphthoic acid (60%), terephthalic acid(20%), and aminophenol (20%)) produced by Hoechst Celanese Co. Because of the high nematic transition temperature of VB (285°C), nylon 66 (Topramid 2021, Hyosung T&C Co., Korea) whose processing temperature is around 280°C was used as the matrix polymer. Maleic-anhydride-grafted PP (MA-PP) was purchased from Honam Chemical Co. (Korea). Its maleic anhydride/ acid content is reported as ca 1 wt%.

2.2. Instruments

2.2.1. Blending and extrusion

The pellets of nylon 66 and Vectra B were dried in a vacuum oven at 120°C for at least 24 h before use. MA-PP was dried in a vacuum oven at 100°C for 24 h. The TLCP content was kept at 20 wt%. The dried VB, nylon 66, and MA-PP were mixed in a container before blending in the extruder. Blending was carried out in a 42 mm Brabender twin-screw extruder (AEV651) at a fixed rotation speed of 10 rpm. It was equipped with a pulling unit imparting different draw ratios (DR), where DR is defined as the diameter at die exit divided by the diameter far down stream, but a high draw ratio was not applicable because of the instability of the nylon extrudates. The extrusion temperatures of the feeding zone/transporting zone/melting zone/die were set as 140/290/290/290°C, respectively.

2.2.2. Thermal properties

Differential scanning calorimetry (DSC) studies of the thermal property characteristics were performed on a DuPont 910 DSC controlled by a 9900 thermal analyzer. Every thermogram was repeated at least twice to verify the reproducibility of the measurements. A DuPont 2000 thermal gravimetric analyzer was also used to observe the degradation of samples. The heating rate was 10°C min^{-1}, and the samples were heated up to 800°C. Dynamic mechanical thermal analysis (DMTA) of the blends was carried out with a Polymer Laboratories Dynamic Mechanical Thermal Analyzer (Model 2) at a frequency of 1 Hz. The dynamic tensile mode was used.

2.2.3. Scanning electron microscopy

Scanning electron microscopy (SEM) observations of the composite samples were performed on a Hitachi S-2200C model. The fractured surfaces of the blends were prepared by cryogenic fracturing in liquid nitrogen followed by a coating with gold in an SPI sputter coater. The morphology was determined using an accelerating voltage of 15 keV.

2.2.4. Wide-angle X-ray scattering (WAXS)

The scattering patterns of the blends and the neat polymers were measured in the symmetrical transmission mode with a RINT DMAX 2000 (Rigaku, Japan) diffractometer. The diffractometer was equipped with an automatic monochromator, step-scan facilities, and a film/fiber stretching accessory. The sample was exposed to Cu Kα radiation. The beam conditions were 36 Kv and 100 mA. The intensity of the scattered radiation was measured with a scintillation counter along the equatorial axis. The sample to receiving slit distance was 76 mm. The 2θ axis was scanned from 10° to 35° at a rate of 10 ° min^{-1} in steps of 0.02°.

2.2.5. Rheometry

Rheological properties of the blends and pure resins were measured using a Rheometrics Dynamic Spectrometer (RDS 7700, Rheometrics, U.S.A) on which a 25 mm or 50 mm diameter parallel plate was mounted. Frequency range was set at 0.1–500 rad s^{-1}. Plate gap was set as 1.2 mm. Before the measurement, the samples were prepared using a compression moulder. Measurement was carried out under the nitrogen atmosphere. Rheological measurement was also carried out using a capillary viscometer RH7(Rosand, England) at 290°C. The capillary was 1 mm in diameter and had a length-to-diameter ratio of 32.

2.2.6. Mechanical properties

Testing of the mechanical properties of the blends was undertaken using an Instron Universal Testing Machine (model 4204) at a constant temperature. A gauge length of 30 mm and a crosshead speed of 10 mm min^{-1} were used. All the reported results are averages of at least seven measurements.

3. Results and discussion

3.1. Thermal properties

The results from the DSC scans for the binary and ternary blends are presented in Fig. 1. The thermal properties of the blends are summarized in Table 1. The glass transition temperature, T_g, was evaluated by DSC and then related to the DMTA point at which tan δ is a maximum. Before the analysis of the ternary blends, binary blends of nylon 66 and VB were studied. The T_g of nylon 66 is known to be 70°C and that of VB to be 142°C. The melting endotherm of VB is not apparent because of its small heat of fusion. It is not clear from the DSC thermograms whether the VB phase forms its own domains or is mixed in the nylon 66. The binary blends display multiple peaks. This phenomenon

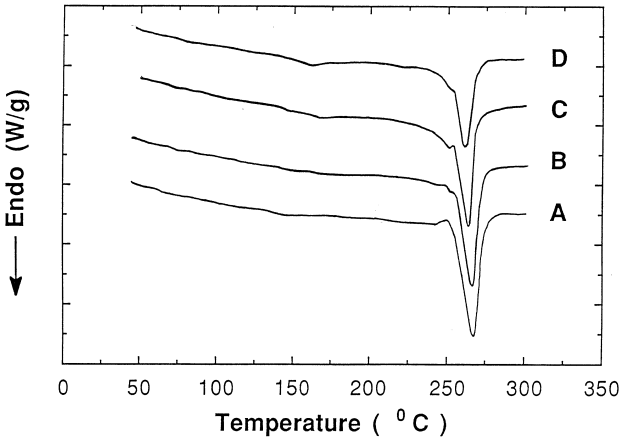

Fig. 1. DSC thermograms of melting behavior of nylon 66 and the blends: (A) nylon 66, (B) binary blend, (C) 2% MA-PP-added ternary blend, (D) 5% MA-PP-added ternary blend.

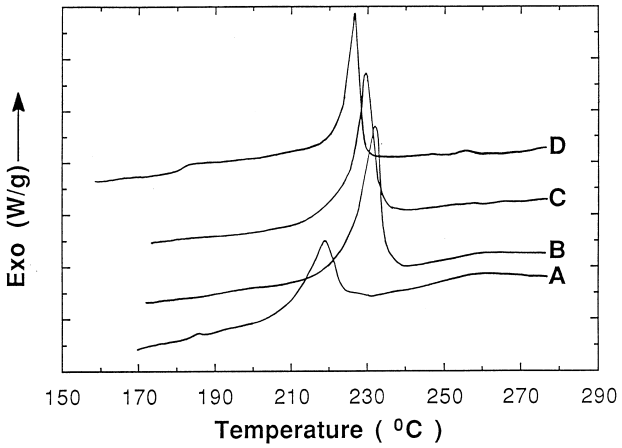

Fig. 2. DSC thermograms of cooling process for nylon 66 and blends: (A) nylon 66, (B) binary blend, (C) 2% MA-PP-added ternary blend, (D) 5% MA-PP-added ternary blend.

can be explained by the existence of different kinds of crystallization processes [16]. A more perfect crystal population has a higher melting temperature at the main peak. The smaller secondary crystals are less perfect and melt to form the secondary peaks. The appearance of multiple melting peaks implies that mixing with VB affects the crystallization process of nylon 66. The recrystallization peaks which appear upon cooling the various blends are shown in Fig. 2. In each case, the samples were held at 300°C for 2 min after heating and then cooled at a rate of 10°C min^{-1}. The pure nylon 66 shows a crystallization-point maximum of about 216°C, similar to that reported for such systems [15]. This maximum shifts quite strongly with the addition of VB. It appears from the melting and the crystallization data that the TLCP phase acts as a nucleating agent. Though TLCP phase affects the crystallization rate of nylon 66, it does not seem to change the crystallization structure as seen from the X-ray spectra. The maximum of tan δ from DMTA is shown in Fig. 3. The T_g of nylon 66 is 78°C and the peak at 145°C is assigned to that of VB. The T_g values obtained from dynamic mechanical analysis are higher than those obtained from thermal analysis. Such a difference is reasonable when one takes the features of these measuring techniques into consideration. The appearance of separate T_gs indicates that nylon 6 and VB are immiscible.

In the ternary blends, the appearance of minor melting peaks in addition to the major melting transition of nylon 66 around 263°C indicates that addition of MA-PP also affects the crystallization process of nylon 66 (Fig. 1). The melting temperature (T_m) of nylon 66 does not show a remarkable variation with MA-PP addition. The enthalpy of crystallization does not change, but the crystallization-peak temperature shifts to a lower temperature with the addition of MA-PP (Fig. 2). This is ascribed to the added MA-PP reacting with VB and nylon 66 to produce a compatibilizer (Scheme 1) which makes the blend more homogeneous [13,14]. This supports the conclusion that VB, the added MA-PP, or both are acting as a nucleating agent. The initiation temperature of nylon 66 crystallization decreases with excess MA-PP addition. Changes in the crystallization process are believed to occur because of altered nucleation and growth conditions in the ternary blends. Excess MA-PP may form a separate phase, which can act as an impurity in the blend. More detailed characterizations are in progress. Fig. 3 shows that addition of MA-PP shifts the T_gs of nylon 66 and VB toward each other. This shift of the T_gs means that nylon 66 and VB become more compatible in the ternary blend. With the addition of more MA-PP, the T_gs move to lower temperatures, as well as moving towards each other. In earlier works, we ascribed the compatibilizing

Table 1
Thermal properties of the blends

MA-PP	T_m (°C)	ΔH_f (J/Ny66 g)	T_{cm}[a] (°C)	T_{ci}[b] (°C)	ΔH_c (J/Ny66 g)	ΔT[c] (°C)
Nylon 66	264.5	69.01	216	235	70.77	29.5
Binary	264.5	86.92	233	235	74.69	29.5
2% MA-PP	263.4	87.87	231	233	77.84	30.4
5% MA-PP	262.7	88.25	227	230	84.44	32.7

[a] Crystallization peak temperature.
[b] Crystallization intiation temperature.
[c] Temperature difference between the melt peak temperature and the crystallization initiation temperature.

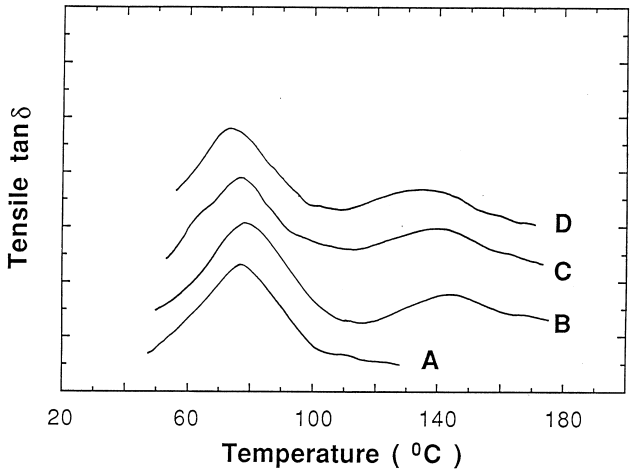

Fig. 3. Normalized tan δ versus temperature for binary and ternary blends: (A) nylon 66, (B) binary blend, (C) 2% MA-PP-added ternary blend, (D) 5% MA-PP-added ternary blend.

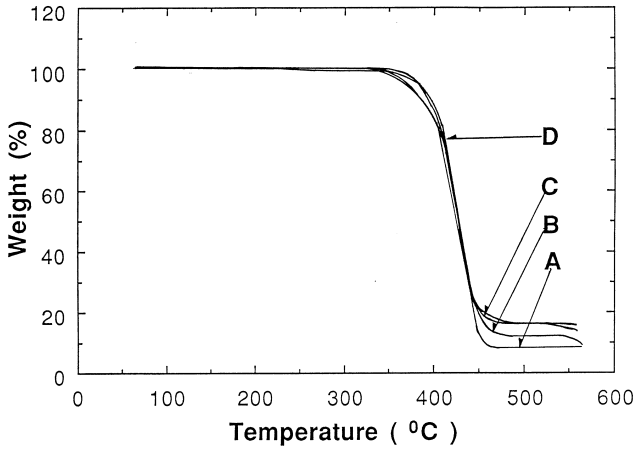

Fig. 4. TGA thermograms of nylon 66 and blends: (A) nylon 66, (B) binary blend, (C) 2% MA-PP-added ternary blend, (D) 5% MA-PP-added ternary blend.

action to the compatibilizer produced in the blending process by chemical reactions between the maleic-anhydride groups and the amine groups of both nylons and TLCPs and/or also some (end) functional groups of TLCP [14,15]. The same reaction is believed to occur between MA-PP and nylon 66 or VB phase (Scheme 1).

An assessment of the thermal degradation characteristics of the neat nylon 66 and blends was made by thermogravimetric analysis (TGA). TGA thermograms of the binary and ternary blends are shown in Fig. 4. No remarkable difference was observed in the thermal degradation behaviors of the binary and the ternary blends. The maximum decomposition temperature, defined as the temperature of the maximum weight loss, was nearly identical for the neat polymer and the blends (around 445 ± 1.5°C).

3.1.1. Rheological properties

The flow curves of the pure components and the ternary blend are presented in Fig. 5. A general feature related to the frequency response is the Cox-Merz rule, whereby the curve of the complex viscosity as a function of frequency should coincide with that of the steady-state viscosity vs the shear rate. The Cox-Merz rule, invariably obeyed by ordinary polymeric liquids, does not generally hold true in TLCPs, because of their long relaxation time [17]. Hence, the complex viscosity of the blend vs the frequency is different from the steady-state viscosity vs the shear rate. It can be conjectured that the complex viscosity value will be higher than the steady-state viscosity since the TLCP phase in the oscillatory mode will be in a partially relaxed state, which makes the system similar to a heterogeneously filled system [14]. The viscosity of VB is higher than that of nylon 66. The processing shear rate (apparent shear rate) was about 40 s^{-1}, and VB has a viscosity nearly one order of magnitude higher than that of nylon 66. The viscosity of the blend in the investigated shear-rate range was lower than those of the neat polymers. This is similar to the results for nylon 6 and nylon 46 blends [13,14]. Thus, the role of TLCP as a processing aid is vividly seen. Ternary blends show

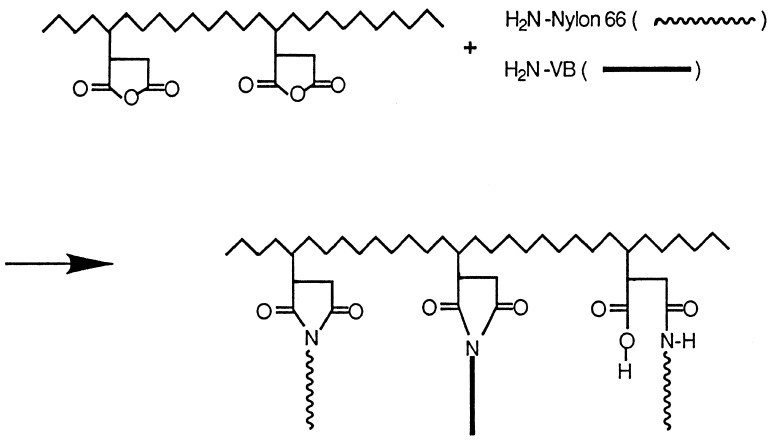

Scheme 1. Reaction between MA-PP and Nylon 66 or VB.

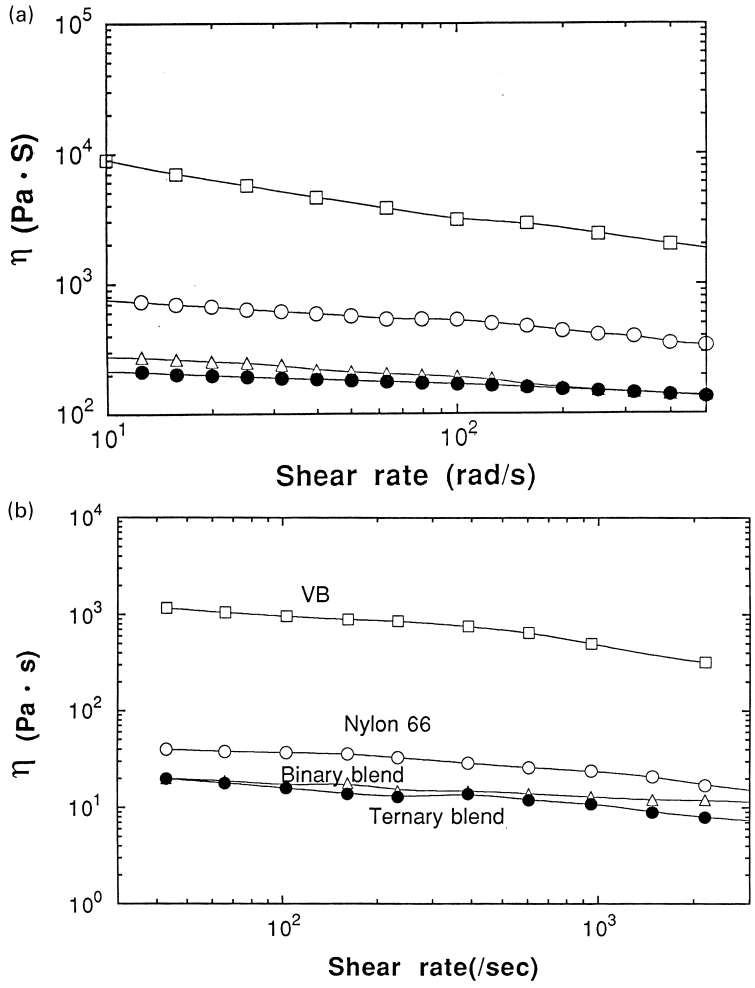

Fig. 5. (a) Dynamic viscosity versus frequency at 290°C (b) Viscosity–shear rate relationship at 290°C: (○) nylon 66, (□) VB, (△) binary blend, (●) 2% MA-PP-added ternary blend.

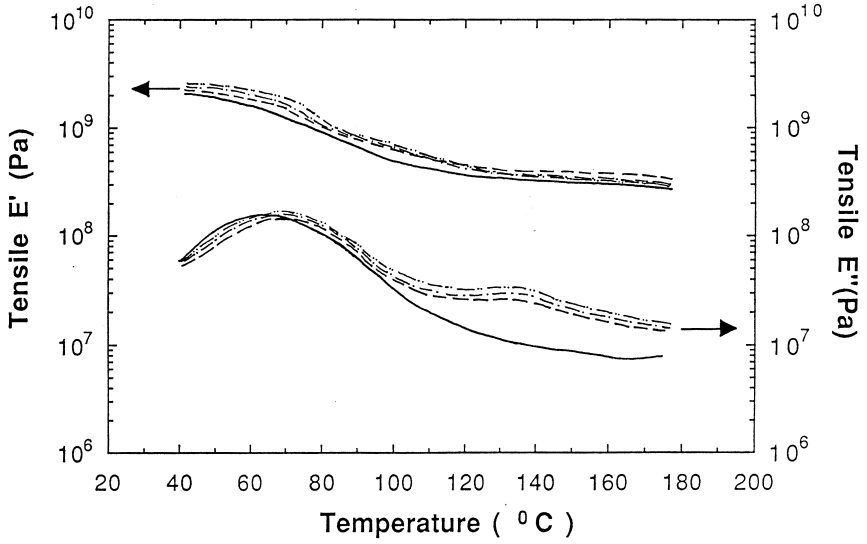

Fig. 6. DMTA measurements of storage moduli (E′) and loss moduli (E″). (—) nylon 66, (——) binary blend, (– · –) 2% MA-PP-added ternary blend, (– · · –) 5% MA-PP-added ternary blend.

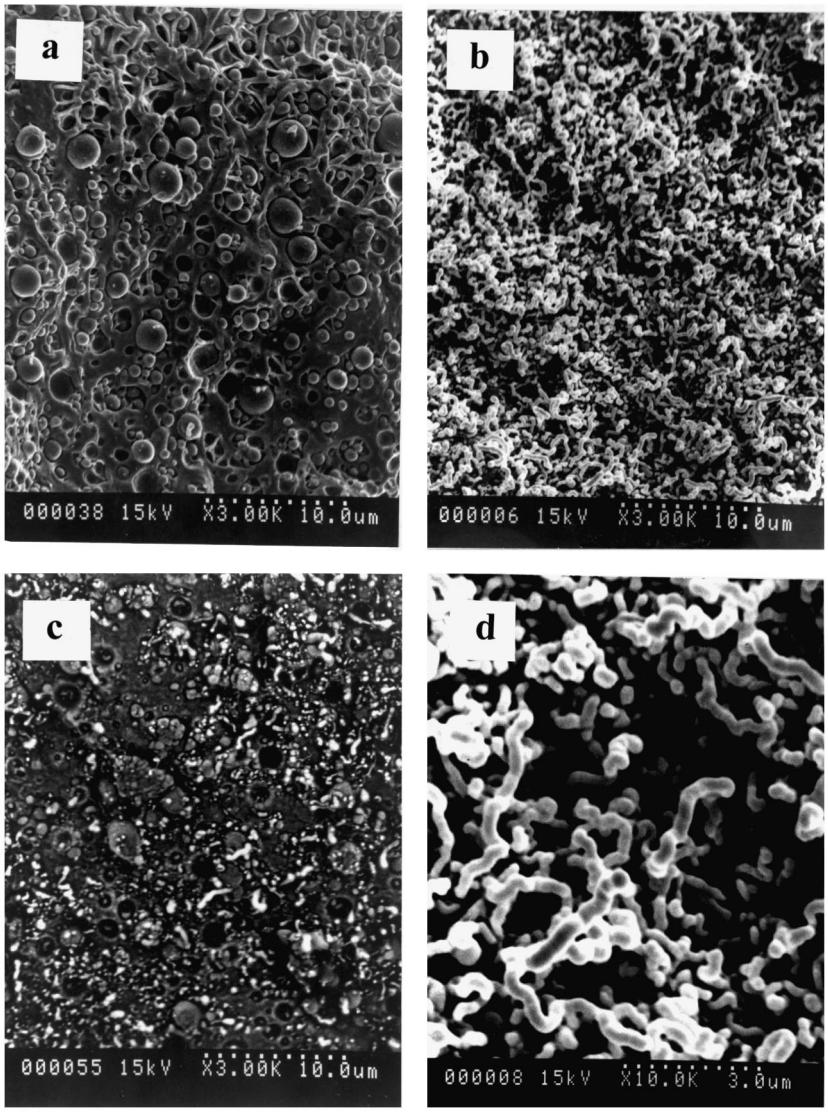

Fig. 7. SEM photographs of fractured surfaces (a) binary blend (b) 2% MA-PP-added ternary blend (c) 5% MA-PP-added ternary blend (d) enlargement of (b).

viscosities even lower than those of binary blends. The reduced viscosities of blends containing TLCP have been attributed to the interlayer slip of the phases for two different reasons: Firstly, incompatibility between the two phases and secondly, the formation of elongated fibrils of the TLCP phase, which tend to lubricate the melt. Both are reasonable explanations, judging from the fact that elongated structures and spherical structures were observed in the SEM micrographs, as will be shown later. Though more effective in the case of fibrils that arise from elongational flow than for the spherical particles often seen in blends undergoing simple shear flow, the fibrillation of TLCP in the nylon 66 matrix is unusual on account of the very low viscosity of the nylon 66 matrix, which cannot deform the spherical droplets of the dispersed TLCP phase in shear flow. This is ascribed to the effect of MA-PP which reacts with VB and nylon 66 to form a kind of graft copolymer that acts at the interface as a compatibilizer (Scheme 1). We have observed that maleic-anhydride-attached EPDM (ethylene-propylene-diene terpolymer) has a similar effect on the blends of VB and other nylons (nylon 6 [14] and nylon 46 [13]). The storage moduli and the loss moduli of nylon 66 and blends are shown in Fig. 6. The storage moduli of the blends show a marked increase compared with those of pure nylon 66 over the entire range of temperatures, especially at temperatures above the T_g of nylon 66. The storage moduli of ternary blends are lower at high temperature than those of the binary blends because of the low modulus of MA-PP. The shift of the primary peak and its expansion to high temperature side in the blends means that the micro-Brownian motion of the amorphous chains of nylon 66 suffers a greater restraint because of the surrounding amorphous chain segments; this has been noted by others [18].

3.1.2. Morphologies of the blends

In an effort to provide more support for the compatibility

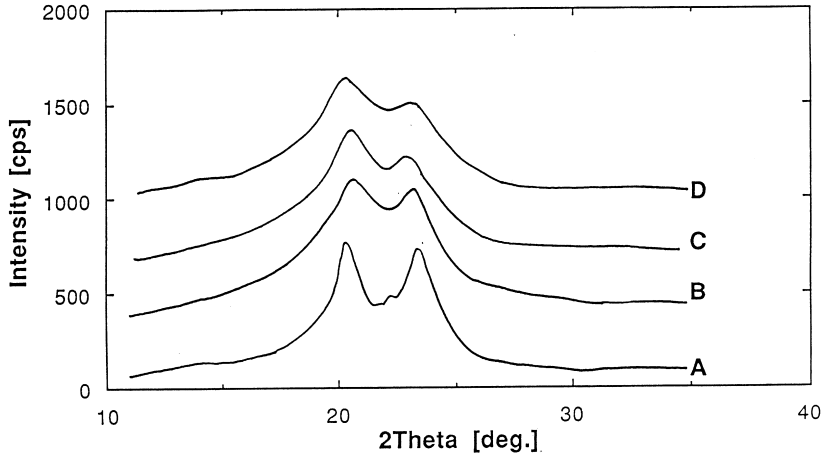

Fig. 8. WAXS spectra of nylon 66, binary and ternary blends. (A) nylon 66, (B) binary blend, (C) 2% MA-PP-added ternary blend, (D) 5% MA-PP-added ternary blend.

of the ternary blend, the morphologies of binary (nylon 66/ VB) and ternary (nylon 66/ VB/ MA-PP) blends were investigated. SEM micrographs of the fractured surfaces of binary blends are shown in Fig. 7. These blends have a similar draw ratio of ca 1.6. In the binary blend (Fig. 7a), void formation resulting from phase separation, a dispersed spherical phase, and poor adhesion between the TLCP and the matrix are observed. The mechanical properties of the binary blend are poor as a result of this morphology. In the binary blend of nylon 66/VB, the TLCP domains are relatively large because of immiscibility, thereby leading to poor dispersion. The micrographs also demonstrate poor adhesion between the two phases, which leads to an open ring hole around the TLCP domain while TLCP is pulled out during the fracture of the samples. The ternary blend surface (Fig. 7b) shows a different morphology. The size of the dispersed phase is noticeably reduced. The fractures are seen to occur within the strands in the ternary blend when 2% MA-PP is added. There is no open ring hole around the TLCP domain, reflecting better adhesion between the two phases. Furthermore, the VB phase shows fibril shapes which are uniformly distributed and which are finer than those in the VB phase of the binary blends (Fig. 7 b and d). When 5% MA-PP is added, a complicated morphology appears (Fig. 7c). Fine TLCP fibril shapes are still observable, but some have been incorporated into large domains. Excess levels of MA-PP seem to induce coagulation or flocculation of the dispersed TLCP phase. This is similar to what we observed in the ternary-blend morphologies of VB/Poly(ether imide)/Poly(ester imide) (PEsI) where poly(ester imide) was used as a compatibilizer [19]. When the proper amount of PEsI was added, fine and uniform microfibrils of VB were observed, while excess amounts of PEsI lead to flocculation or coagulation of the dispersed TLCP phase. From emulsion studies, flocculation of the dispersed phase is known to occur because of strong interparticle interactions, and the quantity of surfactant required to fully cover an interface is related to many variables [20]. In a previous study, we observed that an optimum amount of compatibilizer exists for achieving uniform dispersion and fibrillation [19]. Instead of size reduction, excess compatibilizer coalesces the dispersed TLCP phase. The coalescence of the TLCP phase results in poor dispersion of the TLCP phase, hence reducing the interfacial area between the matrix and TLCP phase. Excess levels of compatibilizer coalesce the TLCP particles before strands are formed. Even the produced fiber domains, some of which were pulled out (see the marked big holes in Fig. 7c), are not homogeneous.

The WAXS patterns of extrudates are shown in Fig. 8. The bottom curve is that of nylon 66. The diffraction patterns of the extrudates change with the mixing of VB and the addition of MA-PP. The diffraction peak at 23.5° becomes less intense with the addition of VB and becomes less intense and broader with MA-PP addition. The diffraction patterns of VB differ significantly from those of nylon 66. Obviously, the crystalline phase in the extrudates has been altered by the processing conditions, but weak peaks do not allow for more definite interpretation because of low intensity.

It should be emphasized again that almost no drawing was done (the draw ratio was ca 1.6) in order to verify the effect of PP-MA on the compatibility and the morphology of the binary blend. The shear rate was at a low level (about $40\ s^{-1}$) where the viscosity of nylon 66 was much lower than that of VB. Weak drawing was inevitable to prevent the extrudate from sagging down under the force of gravity. The fibers in Fig. 7b and d have a large aspect ratio. Finer dispersion and better adhesion clearly demonstrate the compatibilizing effect of MA-PP. The submicron-sized fibrils in Fig. 7b manifest the effect of PP-MA. The compatibilizer yields not only a reduction in the interfacial tension but also better adhesion which invokes effective stress transfer at the interface. The final shape of the dispersed phase is a dynamic equilibrium between the shear stress and the compatibilizing action. Needless to say, thermoplastics of high viscosity possess sufficient melt strength to withstand

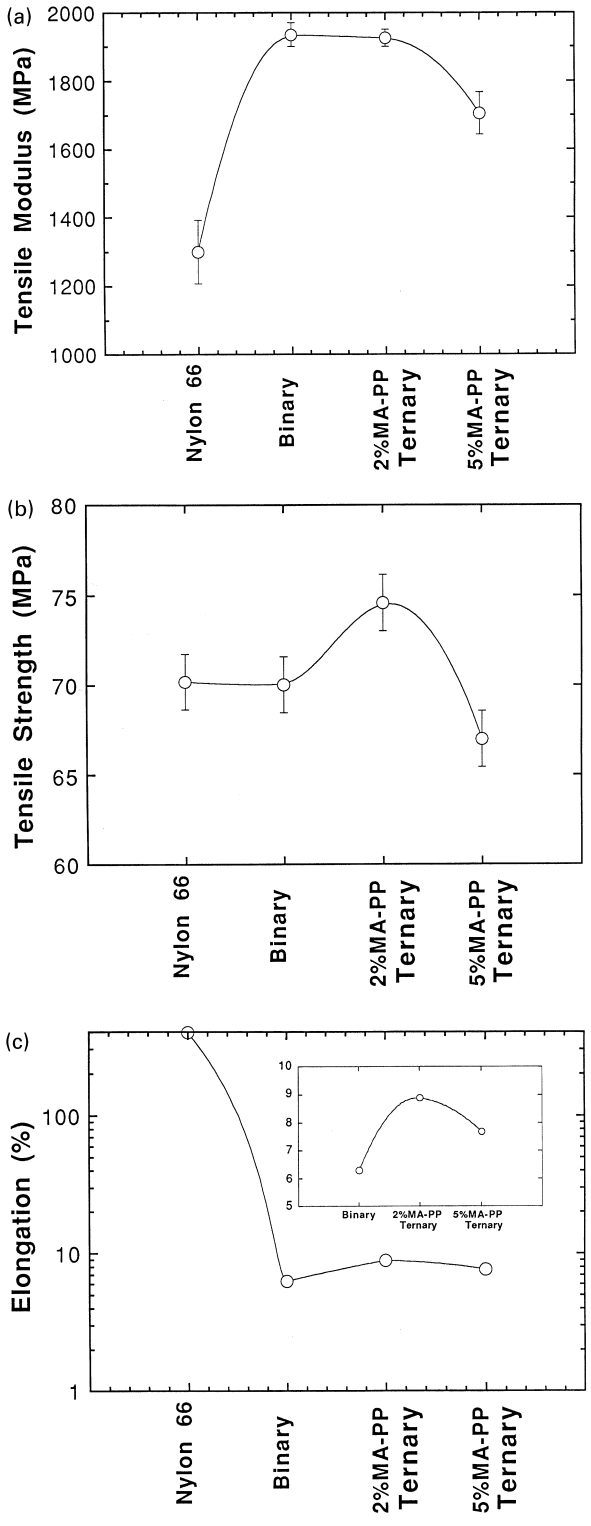

Fig. 9. Mechanical properties of nylon 66 and blends. (a) tensile modulus and (b) tensile strength (c) elongation at break. The inset shows the maximum when 2% MA-PP was added.

strong flow (elongational flow) that easily deforms small droplets; this is not possible with weak flow (shear flow). As verified experimentally by La Mantia et al. [10,11] for a nylon 6 blend with VB, the nylon 6 matrix does not easily deform the TLCP droplets in spite of high elongational deformation (a draw ratio of 100). Therefore, efficient stress transfer by improved adhesion at the interface is the only practical way to achieve the deformation of TLCP droplets in the nylon matrix, even without high elongation. Depending on the compatibilizing action at the interface, relatively small droplets can also be deformed (Fig. 7b).

3.1.3. Mechanical properties

The morphological differences between blends with and without MA-PP definitely affect their respective physical properties. The tensile strengths and tensile moduli of binary and ternary blends are shown in Fig. 9. The tensile modulus increases with the addition of hard TLCP. In spite of morphological development, the modulus of the 2% MA-PP-added ternary blend did not show much improvement (Fig. 9a) over that of the binary blend. In fact, it was reduced for a 5% MA-PP-added system. This is attributed to MA-PP hampering the crystalline-phase development of nylon 66. Also, addition of low-modulus MA-PP contributes to the modulus decrease. However, the tensile strength shows a slight improvement over that of the binary blend (Fig. 9b). When excess MA-PP was added, the inhomogeneity of the structure cause the mechanical properties to deteriorate.

The elongation of the 2% MA-PP-added ternary blend is better than that of the binary blend (Fig. 9c). For immiscible, reinforced composites, the elongation generally decreases when the tensile modulus and the tensile strength increase [21]. Generally, the higher the modulus of the composite, the harder the composite and the lower the elongation. Our results differ from this expectation. This is ascribable to the role of the compatibilizer. The simultaneous increases in tensile strength (or tensile modulus) and elongation can be explained by improved adhesion due to the compatibilizer at the interface and by the micromechanism for formation of fractures in the composite. Fibrous composites can fail during monotonic loading as a result of a number of competing fracture micromechanisms, such as fiber breakage, matrix cracking, and fiber pull-out [22]. Depending on the form in which the stored elastic strain energy in the fiber is released, and on the strength and the toughness of the fiber, the fiber–matrix interface, and the matrix itself, brittle fracture can result from the earliest failure event (a matrix crack, for instance) and the distribution of flaws. A short fiber (or undeformed droplet) is pulled-out if the force on the fiber is sufficient to cause some debonding. In contrast, for long fibers embedded in a matrix under tensile stress, the fraction of pulled out fibers, rather than broken ones, approaches zero as the fiber length increases. This means that such fibers must fracture along a common crack plane or fracture into smaller segments before being pulled out of the matrix (see fig. 6 of [19]). Examination of the fracture surface of the composite (Fig. 7) reveals broken fibers of various lengths protruding above the fracture surface of the matrix. These breaks occur because of variations in strengths of the fibers at weak points beneath the surface of the cracked

matrix. When a fiber fractures, in order for the new surfaces to move apart, the matrix must crack or plastically deform, and the next fiber must fracture in the crack plane or beyond the crack plane and then be axially pulled out of the matrix [22]. Matrix plastic deformation and fiber pull-out require additional energy input to the material and provide a means of dissipating the energy decrement necessarily associated with fracture. Since the frictional shear force opposes any force applied to extract the fiber, work must be done in overcoming this frictional force. A compatibilized composite has a greater frictional shear force resulting from strong adhesion at the interface between the matrix and the fiber, and requires more energy to pull out the strands. As a result, the tensile strength of the system increases. Provided the strand still maintains contact with the sheath of the matrix surrounding it, work must be done in pulling the fiber fragments against the restraining frictional force at the fiber–matrix interface. If the fiber does not maintain contact with the sheath of the matrix, the fibers can be easily pulled out and the elongation cannot be increased. However, additional energy must be expended to break the strong adhesion at the interface for the compatibilized system. Fibers will not simply be debonded. A fiber sustains its fibril shape over the gap between crack surfaces until additional energy is supplied. This allows the blends containing a small amount of compatibilizer to gain a higher elongation at break than a non-compatibilized system does. Excess compatibilizer, however, brings about the coalescence of the dispersed phase. As a result of poor dispersion, the tensile strength and the modulus decrease. The elongation also decreases because the total contacting area is decreased and the energy restraining the crack is also decreased. The elongation at break of all blends decreases markedly, compared to that of nylon 66, because of the loss of ductility of the nylon 66 matrix. The hard and strong, but inextensible, strands of VB restrain the ductile deformations of the polymer composite to give low elongation. The improvement of the tensile strength upon addition of MA-PP is ascribed to better adhesion at the interface and to fine fibril formation. The low elongation at break, compared to that for nylon 66, is partly ascribable to the degradation of MA-PP. Degradation of MA-PP, which is fractured first under a tensile force, produces the same effects as do defects in the blend.

4. Conclusions

We have investigated the possible deformation and the fibril-shape formation of TLCP (VB) in a nylon 66 matrix whose viscosity is lower than that of VB by adding a small amount of a functionalized polypropylene whose functional group(maleic anhydride) can react with end groups (amines) of nylon 66 and VB to produce graft copolymers that act as a compatibilizer at the interface. When a proper amount of the compatibilizer is added, fine strands are formed in the ternary blend system, even without strong elongational drawing. Good adhesion at the interface is believed to promote efficient stress transfer to deform the TLCP droplets which are in the melt state at the processing temperature. This result corroborates the observation that the interfacial adhesion and the sizes of the dispersed droplets are as much decisive factors as the ratio of the viscosity of the TLCP to that of the isotropic polymer in determining the deformation and the structure development of the TLCP phase. Scanning electron micrographs demonstrate that, if the proper amount of compatibilizer is added, elongation and the orientation of the TLCP phase to form a strand structure can occur even when the viscosity of the matrix polymer is much lower than that of the dispersed TLCP phase.

The mechanical properties (elongation, as well as tensile strength and modulus) are improved when the proper amount of MA-PP is added, which enables improved adhesion at the interface. The loss of nylon 66's ductility as a result of the addition of VB is ascribed to the incompatibility of those two, but the compatibility can be improved by the addition of MA-PP. It may also be partly attributed to the degradation of the added MA-PP at high temperatures. When excess MA-PP was added, the inhomogeneous structure caused the mechanical properties to deteriorate. As we noted in our previous study [14,19], using the optimum amount of the compatibilizer is the key to obtaining the best morphology and, hence, the best mechanical properties.

Acknowledgements

The authors appreciate the financial support from the Korea Institute of Science and Technology (KIST) under Grant No. 2E14630. We would like to thank Dr. Hak-kil Kim at Hyosung T&C Co. for providing the nylon 66 resin. Special thanks to Dr. Seung Sang Hwang for helpful discussion about thermal properties and X-rays.

References

[1] La Mantia FR, editor. Thermotropic liquid crystal polymer blends. Lancaster: Technomic Publishing, 1993.
[2] Isayev AI, Limtasiri T. In: Lee SM, editor. International encyclopedia of composites vol. III. New York: VCH Publishers, 1990.
[3] Williams DJ. Adv Polym Tech 1990;10:173.
[4] Handlos V, Baird DG. J Macromol Sci, Rev 1995;35(2):183.
[5] Carfagna C, Amendola E, Nobille MR. In: Lee SM, editor. International encyclopedia of composites vol. II. New York: VCH Publishers, 1990.
[6] Crevecour G, Groeninckx G. Polym Comp 1992;13(3):244.
[7] Grace HP. Chem Eng Commun 1982;14:225.
[8] Delaby I, Froelich D, Muller R. Macromol Symp 1995;100:131.
[9] Weiss RA, Huh W, Nicholais L. In: Zacharides AE, Porter RS, editors. High modulus polymers. New York: Marcel Dekker, 1988.
[10] La Mantia FP, Saiu M, Valenza A, Paci M, Magagnini PL. Europ Polym J 1990;26:323.
[11] La Mantia FP, Saiu M, Valenza A, Paci M, Magagnini PL. J Appl Polym Sci 1989;38:583 and Polym Eng Sci 1990;30:7.
[12] Berry D, Kenig S, Siegmann A. Polym Eng Sci 1991;31:451.

[13] Klein N, Selivansky D, Maron G. Polym Compos 1995;16:189.
[14] Seo Y, Hong SM, Kim KU. Macromolecules 1997;30:2978.
[15] Seo Y, Kim KU. Polym Eng Sci 1998;38:596.
[16] Wunderlich B. Macromolecular physics, vol.1. New York: Academic Press, 1973.
[17] Marrucci G. In: Acierno D, Colloyer AA, editors. Rheology and processing of liquid crystal polymers. London: Chapman and Hall, 1996.
[18] Takayanaki M, Ogata M. J Macromol Sci Phys B 1980;17:591.
[19] Seo Y, Hong SM, Hwang SS, Park TS, Kim KU, Lee S, Lee JW. Polymer 1995;36:515 and 525.
[20] Piirma I. Polymeric surfactants. New York: Marcel Dekker, 1992.
[21] Gent AN. In: Eirich F, editor. Science and technology of rubber, Chapter 10. New York: Academic Press, 1989.
[22] Beaumont PWR, Schultz JM. Failure analysis of composite materials (Delaware composite design encyclopedia, Vol. 4). Lancaster: Technomic, 1990.